



## Rejuvenation Heat Treatment of Nickel Base Superalloy Grade GTD111 after Long-term Service via Taguchi Method for Optimization

S. Toocharoen, S. Kaewkuekool, P. Peasura\*

Department of Production Technology Education, Faculty of Industrial Education and Technology, King Mongkut's University of Technology Thonburi, Thailand

### PAPER INFO

#### Paper history:

Received 18 December 2020

Received in revised form 27 January 2021

Accepted 02 February 2021

#### Keywords:

GTD111

Rejuvenation Heat Treatment

Taguchi Method

Hardness

Microstructure

### ABSTRACT

This research describes an optimization and rejuvenation of the heat treatment process for a nickel base superalloy grade GTD111 after long-term service. The aging heat treatment variables examined in this study included primary aging temperature, primary aging time, secondary aging temperature, and secondary aging time. The resulting materials were examined using Taguchi method design of experiments to determine the resulting material hardness test and observed with the hot tensile test, scanning electron microscopy, and energy dispersive X-ray spectroscopy. The experimental results showed what happens following optimization with the heat treatment parameters of a primary aging temperature of 1120 °C, primary aging time of 3 h, secondary aging temperature of 845 °C, and secondary aging time of 24 h. The material, after rejuvenation heat treatment via optimization with  $\gamma'$  particle characteristics, had a coarse square shape, spherical shape of  $\gamma'$ , and fine  $\gamma'$  precipitate distributed on the parent phase, which affects the mechanical properties of the material. fine  $\gamma'$  precipitate distributed on parent phase, which affects the mechanical properties of the material.

doi: 10.5829/ije.2021.34.04a.22

## 1. INTRODUCTION

Nickle base superalloys grade GTD111 are used extensively in the industry for high-temperature applications such as the production of the gas turbine. The GTD111 grade is used for high-temperature applications because it has good mechanical properties and is resistant to corrosion and fatigue at high temperatures. Esanab et al. [1] conducted a data-based investigation on the performance of an independent gas turbine and found that turbines are one of the most prominent technologies being adopted in producing electricity from natural gas; this part is attacked by hot gas. The mechanical properties of superalloys create a multiphase, such as precipitation strengthening of  $\text{Ni}_3(\text{Al,Ti})$  or  $\gamma'$  phase and carbide phase. The particles disrupt the movement of the dislocation; this increases the strength of the material [2,3].

The microstructural characteristics of the alloy would be normally degraded, resulting in poorer mechanical

properties after long-term service and finally leading to failure of components. These increasingly extreme operating environments accelerate the aging process in materials, leading to reduce performance and hot corrosion failure. The cause of blade trailing edge failure is thermal stress leading to thermal fatigue according to Perrut et al. [4] and Salehnasaba et al. [5]. Zhangab et al. [6] studied creep behavior and deformation mechanisms of a novel directionally solidified Ni-base superalloy and found that to repair the material, it is necessary to restore its initial properties and the original microstructure first. The alloy gains its appropriate microstructure and high-temperature strength through a precipitation hardening mechanism. Heat treatment is the way to improve this material. Kim et al. [7] studied transient liquid phase bonding of  $\gamma'$ -precipitation strengthened Ni-based superalloys. Rezaie et al. [8] studied the effects of temperature and pressure in the HIP process on mechanical properties and found that homogenization treatment resulted in a more uniform distribution of the

\*Corresponding Author Email: [prachya.pea@kmutt.ac.th](mailto:prachya.pea@kmutt.ac.th) (P. Peasura)

$\gamma'$  precipitates. This shows that precipitation hardening of  $\gamma'$  precipitates affects the microstructure. In their studies, the heat treatment conditions influenced the size distribution and the microstructure of  $\gamma'$  precipitate, which mainly include solution heat treatment and aging. All the parameters which are important for repair, such as time and the temperature of the heat treatment process, affected the microstructure. In a study on the effect of reheat treatment on microstructure and stress rupture property of a directionally solidified material, Jiang et al. [9] studied temperature and pressure in the HIP process on the mechanical properties of GTD-111 after long-term thermal exposure. Kaplanskii et al. [10] reported an influence of aging and HIP treatment on the structure and properties of NiAl-based turbine blades manufactured by laser powder bed fusion, and Xua et al. [11] studied short-term creep behavior of an additive manufactured non-weldable Ni-base superalloy evaluated by slow strain rate testing.

The method for improving the mechanical properties and microstructure of the GTD111 grade is extremely important. Statistical studying is not used only for data analysis, but primarily for the planning of experiments. Taguchi's method can determine the best combination of factors and interact with the influence behavior of the response variable in the given process. C.D. Pimenta et al. [12] studied the application of Taguchi's method in the investigation of influential heat treatment factors in steel wires. Taguchi's method can be used to create mathematical equations for predicting the mechanical properties of heat treatment. H. Terzioglu [13] analyzed the effect factors of Taguchi's method and its application for the optimization of Ni-base superalloys. G. kartheeka et al. [14] and A. Kumar et al. [15] studied the optimization of residual stresses in the heat treatment process of superalloys. R.M. Dodoa et al. studied multi-response optimization and analysis through Taguchi's method for quenching applications [16]. M. Sobhani et al. [17] and A.S. Canbolata et al. [18] used Taguchi's method for optimization to find the best parameter of experiment. Despite all these studies, no research has been applied to the Taguchi experiment to identify the efficiency of the heat treatment process in improving the mechanical and microstructural properties of GTD 111 after long-term service.

In this study, Ni-base superalloys grade GTD-111 which had been degraded following a long-term service period were used. The heat treatment process was used for rejuvenation in nickel base superalloys grade GTD111. Therefore, the research studied the rejuvenation of materials with heat treatment after long-term use in order for them to be recycled, as well as the effects of applying our experimental design combining Taguchi's design method and the optimization and mathematic model on the mechanical properties and microstructure refurbishment of grade GTD111

materials. The study also examined the effects of heat treatment factors on the GTD111 grade performance characteristics, such as microstructure, hardness, and strength, with the hot tensile test. It is also essential to understand the process behavior followed by a proper selection of heat treatment factors of critical importance to achieve satisfactory results in terms of extending the useful life of the material, as well as a significant cost reduction, and be able to apply the material in the gas turbine engine industry with the highest quality and efficiency.

## 2. MATERIALS

**2.1. Material** GTD111 after long-term service was used for the test specimen shown in Figure 1. The specimens were 5.00 mm thick. The details of the chemical composition of the GTD111. GTD111 are provided in Table 1.

### 2.2. Rejuvenation Heat Treatment Process

This research examined the rejuvenation of used GTD111 material via the heat treatment process. The heat treatment process used to improve the microstructure and mechanical properties has 3 steps: first, solution heat treatment, second, primary aging, and third, secondary aging. For solution aging the research was controlled as 1200 °C at 4 hours for every sample. The research studied two factors, the influence of primary aging and secondary aging, because both factors affect the  $\gamma'$  size and the mechanical properties of the material. The sequence of the heat treatment process can be seen in Figure 2.

### 2.3. Design of Experiment

The experimental design through Taguchi's method is the application of the experimental design to control factors, uncontrollable



**Figure 1.** Nickel base superalloys grade GTD111 after long-term service

**TABLE 1.** Chemical composition of the GTD111 by weight (%)

Ni	Cr	Co	Ti	W	Al	Ta	Mo	Fe	C	B
Bal.	13.5	9.5	4.75	3.8	3.3	2.7	1.53	0.23	0.09	0.01

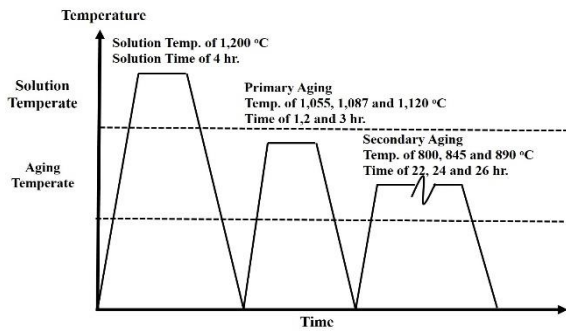


Figure 2. The sequence of the rejuvenation heat treatment process

factors or noise factors, all of which are variables that serve as the source of variation. It is not possible to eliminate the influence of these variables. Therefore, the main function of Taguchi’s method was to reduce data fluctuations by selecting the control factors. The raw experiment results were converted into a signal to noise (S/N) ratio which is important in finding the right target. To optimize the characteristics of the S/N ratio, it can be divided into 3 types, which are “Small the Better Type Problem”, “Nominal the Best Type Problem”, and “Larger the Better Type Problem”. [18] The benefits of the Taguchi method are that it helps to reduce the number of trials, saves time, reduces trial costs and gives reliable results. The research procedure for the Taguchi’s method experiment is shown in Figure 3.

For the design of the experiment with the Taguchi method, we considered the factors that affect the hardness in the heat treatment process using the L27 (3<sup>4</sup>) orthogonal array. There are 4 input factors, which are primary aging temperature, primary aging time, secondary aging temperature, and secondary aging time, each of which is divided into 3 levels of experiments. A treatment total of 27 is shown in Table 2.

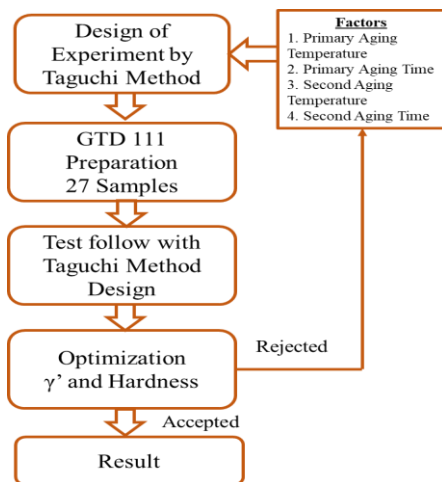


Figure 3. The research procedure of the Taguchi method

TABLE 2. Experimental Taguchi Design

Factors	Symbol	Level		
Primary Aging Temperature	X <sub>1</sub>	1.055	1.087	1.120
Primary Aging Time	X <sub>2</sub>	1	2	3
Secondary Aging Temperature	X <sub>3</sub>	800	845	890
Secondary Aging Time	X <sub>4</sub>	22	24	26

**2. 4. Hardness Test** This research used the Vickers hardness test method. Vickers hardness consists of indenting the test material with a diamond pyramid with a square base and an angle of 136 degrees. The two diagonals of the indentation left on the surface of the material after removal of the load are measured using a microscope, and their average is calculated. The area of the sloping surface of the indentation is calculated. Vickers hardness is the quotient obtained by dividing the kg<sub>f</sub> load by the square mm area of indentation. Hardness was analyzed with the Vickers hardness tester Model MMT-X7 and was determined using a 500 g<sub>f</sub> for dwell time of 10 sec to observe the effects of the heat treatment factors.

**2. 5. Microstructure Test** The specimens were sectioned transversely and polished using standard metallographic techniques. The microstructures were examined and analyzed with an optical microscope (OM). Additionally, scanning electron microscopy (SEM) also used to examine the specimens. Etching was performed using Marble’s reagent (7.5 mL HF, 2.5 mL HNO<sub>3</sub>, 200 mL methanol) for 30 seconds to permit observation of the microstructure with scanning electron microscopy. The microstructures in the γ’ size were examined and analyzed with an ImageJ program.

**2. 6. Hot Tensile Test** The heat treatment samples were hot tensile tested to analyze the mechanical properties of Ni-Base super alloys grade GTD111. The tensile fracture characteristics of the samples with the best mechanical properties of hardness and weakness and mechanical properties of hardness were observed to confirm the critical temperature of high-temperature embrittlement fracture. The specimens were tensile tested at a high temperature of 871 °C [19] with the universal testing machine model HT-8336. The microstructure of the hot tensile specimens was observed by scanning electron microscopy. The dimensions of the hot tensile samples are shown in Figure 4.

**3. RESULT AND DISCUSSION**

**3. 1. Taguchi Method Analysis** The Taguchi method was designed form orthogonal array experiments

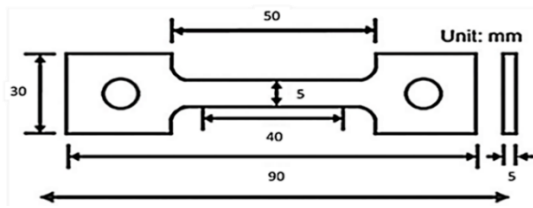


Figure 4. Dimensions of a hot tensile samples

of 27 experiments for 4 factors and 3 levels, considering the factors that affected the average of the interested response, the hardness, and the average signal to noise (S/N) ratio. [17,18] The research divided the Taguchi problem functions into categories, namely, the larger the better type for hardness as calculated from Equation (1). The experimental results showed the hardness and average signal to noise ratio are shown in Table 3. Problem larger is better type:

$$S/N_L = 10 \log \left[ \frac{1}{n} \sum \frac{1}{y_i^2} \right] \quad (1)$$

where  $Y_i$  is the data measured in duplication.  $n$  is the repeated trial number.

The results showed that primary aging temperature ( $X_1$ ) had the highest affected on response for signal to noise ratios in rejuvenation heat treatment process which followed by secondary aging temperature ( $X_3$ ), primary aging time ( $X_2$ ) and secondary aging time ( $X_4$ ), respectively (Table 4). In these experiments, the difference between the average value of each factor is considered a level of the factor.

TABLE 3. Experiment result for hardness based on Taguchi's L27 orthogonal array design matrix

Order	$X_1$	$X_2$	$X_3$	$X_4$	Hardness (HV)	S/N
1	1055	1	800	22	496.40	53.91
2	1055	1	845	24	501.40	54.12
3	1055	1	890	26	499.60	53.97
4	1055	2	800	24	502.90	54.03
5	1055	2	845	26	506.00	54.08
6	1055	2	890	22	498.40	53.95
7	1055	3	800	26	505.50	54.07
8	1055	3	845	22	510.90	54.16
9	1055	3	890	24	501.40	54.00
10	1087	1	800	22	502.90	53.96
11	1087	1	845	24	511.90	54.18
12	1087	1	890	26	502.40	54.02
13	1087	2	800	24	512.30	54.19
14	1087	2	845	26	512.60	54.19

15	1087	2	890	22	507.90	54.11
16	1087	3	800	26	513.30	54.20
17	1087	3	845	22	518.00	54.28
18	1087	3	890	24	514.00	54.21
19	1120	1	800	22	516.50	54.26
20	1120	1	845	24	519.10	54.30
21	1120	1	890	26	515.30	54.24
22	1120	2	800	24	529.50	54.37
23	1120	2	845	26	524.80	54.40
24	1120	2	890	22	512.40	54.19
25	1120	3	800	26	526.80	54.43
26	1120	3	845	22	528.10	54.45
27	1120	3	890	24	517.40	54.22

TABLE 4. Response for signal to noise ratios

Level	$X_1$	$X_2$	$X_3$	$X_4$
1	54.04	54.11	54.16	54.15
2	54.15	54.17	54.24	54.18
3	54.32	54.23	54.10	54.18
Delta	0.29	0.12	0.14	0.04
Rank	1	3	2	4

The results of the variance analysis to test the hypothesis in the research determined the confidence level at 95 percent ( $p$ -value  $< 0.05$ ). The analysis of the experimental results is shown in Table 5. The research found that primary aging temperature, primary aging time, and secondary aging temperature have  $p$ -values  $\leq 0.001$ ,  $0.001$ , and  $0.001$ , respectively, indicating that the 3 factors have a significant ( $p$ -value  $< 0.05$ ) influence on hardness in the heat treatment process.

From Table 6, the coefficient for hardness of the heat treatment of GTD111 shows that primary temperature and secondary temperature have an effect on hardness at 95% confidence level ( $p$ -value  $< 0.05$ ). The heat treatment factors that did not affect hardness were secondary temperature and secondary time. The results indicate that the heat treatment data could be hardness predicted using the model shown in model 2. The  $R^2$ (adj) of the collected data was approximately 83.72%, which shows that the response can be described by the experimental factors.

The regression model for hardness is:

$$Y_{HV} = 220 + 0.279(X^1) + 3.880(X^2) - 0.0362 (X^3) + 0.414 (X^4) \quad (2)$$

**3. 2. Optimization for GTD111 Heat Treatment Process**

The determination of the optimization of **TABLE 5.** Analysis of variance for signal to noise (SN) ratios of hardness

Source	DF	Seq SS	Adj SS	Adj MS	F	P
Primary Aging Temp	2	0.370	0.370	0.185	62.640	0.001
Primary Aging Time	2	0.065	0.065	0.032	11.070	0.001
Secondary Aging Temp	2	0.088	0.088	0.044	15.000	0.001
Secondary Aging Time	2	0.008	0.008	0.004	1.450	0.261
Residual Error	18	0.053	0.053	0.002		
Total	26	0.586				

**TABLE 6.** Estimated model coefficients for hardness

Term	Coef	SE Coef	T	P
Constant	220.150	34.520	6.380	0.001
Primary Temp (X <sub>1</sub> )	0.279	0.026	10.590	0.001
Primary Time (X <sub>2</sub> )	3.883	0.857	4.530	0.001
Secondary Temp (X <sub>3</sub> )	-0.036	0.019	-1.900	0.071
Secondary Time (X <sub>4</sub> )	0.413	0.428	0.970	0.345
R <sup>2</sup> = 86.20%		R <sup>2</sup> (adj) = 83.72%		

4 factors in the heat treatment process is shown in Figure 5, which depicts the relationship of the averages and the response to the factors. The research selected the S/N ratios of the larger the better type for hardness.

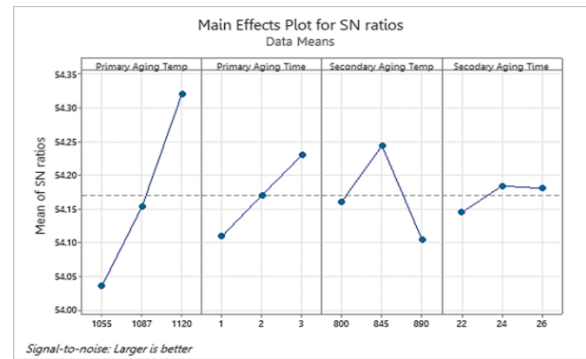


**Figure 5.** Main effects plot for S/N ratios of hardness

For the variation between the factors, the signal to noise ratio (S/N) was calculated following the methodology. The relationship “larger is better” was adopted in this study. The result showed that the highest hardness value was observed at 1120 °C for 3 h in primary aging temperature and primary aging time, respectively. However, the hardness value was decreased with increasing temperature from 845-890 °C which the highest hardness value was observed at 845 °C in secondary aging temperature. The secondary aging time at 24 h. had the highest hardness value which hardness decreased after 24 h. It indicated the change in hardness from graph as a result of over aging.[3-4] The aging heat treatment factors have the highest hardness, shown in Figure 5, with a primary aging temperature of 1120 °C, primary aging time of 3 h, secondary aging temperature of 845 °C, and secondary aging time of 24 h.

Taguchi’s method was analyzed, and the optimization found that a primary aging temperature of 1,120 °C, primary aging time of 3 h, secondary aging temperature of 845 °C and secondary aging time of 24 h result in the maximum GTD111 hardness. Figure 6A depicts the microstructures of the GTD111 grade specimen after long-term service at expanding 50,000 h. For the

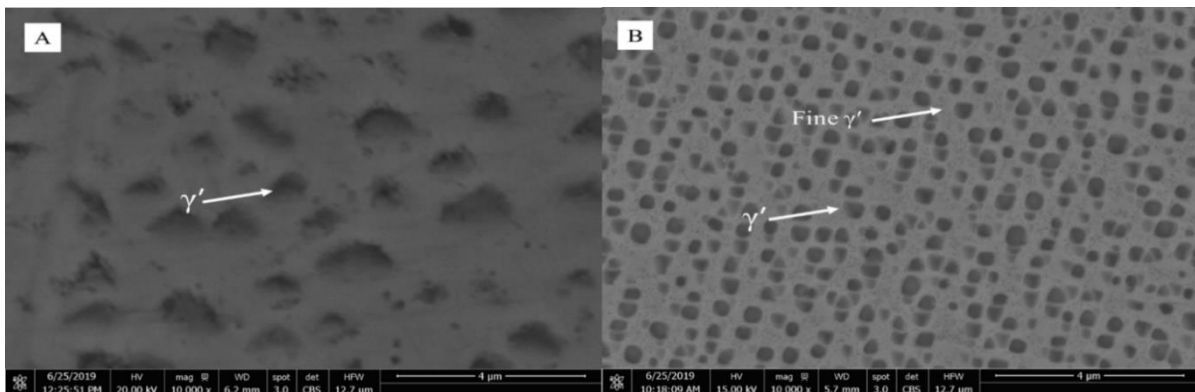


**Figure 6.** SEM image, showing the GTD111 grade. A. after long-term service at expanding 50,000 h. B. primary aging temperature of 1,120 °C, primary aging time of 3 h, secondary aging temperature of 845 °C, and secondary aging time of 24 h

microstructure, an austenite ( $\gamma$ ) phase matrix comprising the main structural and scattered  $\gamma'$  asymmetrical shape was observed in the parent phase specimen with a hardness of 430.30 HV. The optimization condition in Figure 6B shows that the square shapes of  $\gamma'$  and fine  $\gamma'$  precipitates were distributed on the  $\gamma$  phase, which had a  $\gamma'$  size of 0.38  $\mu\text{m}$  and hardness of 530.10. A comparison of the microstructures of the material after long-term service and the aging heat treatment specimens revealed clear differences. There was a reform  $\gamma'$  shape and size increase in density of the square shape  $\gamma'$  and fine  $\gamma'$ , which resulted in increased GTD111 hardness consistent with the research. Rezaiea [20] also reported that the size shape of  $\gamma'$  precipitates and mechanical property was controlled by aging temperature and time. Therefore, the optimization condition was also used in the improvement of the microstructure and hardness of GTD111.

**3.3. Microstructure Analysis** The microstructure was examined via a scanning electron microscope (SEM) and energy dispersive X-ray spectrometer (EDS) of the GTD111. The microstructure showed coarse and fine  $\gamma'$  particle phases with various shapes, including a spherical shape, square shape, and cubic shape of  $\gamma'$  particles.

In Figure 7, where an SEM image shows the microstructure of superalloys grade GTD111 after aging heat treatment, we can see the gamma prime particle ( $\gamma'$  or  $\text{Ni}_3(\text{Al,Ti})$ ) [21] precipitate evenly distributed in the face centered cubic (FCC) or gamma ( $\gamma$ ) matrix [22]. Analyzing the elemental concentrations in the tertiary  $\gamma'$ , EDS as shown in Figure 8 exhibits additional related elements such as Cr Co, containing a large number of elements. The  $\gamma$  phase was decorated with a discontinuous carbide layer scattered throughout the matrix. The carbides were MC (Ta,Ti,W) [21]. The MC carbides were evenly distributed throughout the matrix [21, 9].

The nickel base superalloys were tensile tested, hardness tested, creep tested, etc. to evaluate their mechanical properties. However, as the temperatures increased, the differences between the tensile properties of different alloys almost disappeared. For polycrystalline nickel-based superalloys, there are mainly three strengthening mechanisms, which are  $\gamma'$  precipitate strengthening,  $\gamma$  phase solid solution strengthening, and grain boundary strengthening form carbide. The primary aging temperature of 1120 °C for 3 h and secondary aging temperature of 845 °C for 24 h. Figure 9 A shows the microstructure where the carbide,

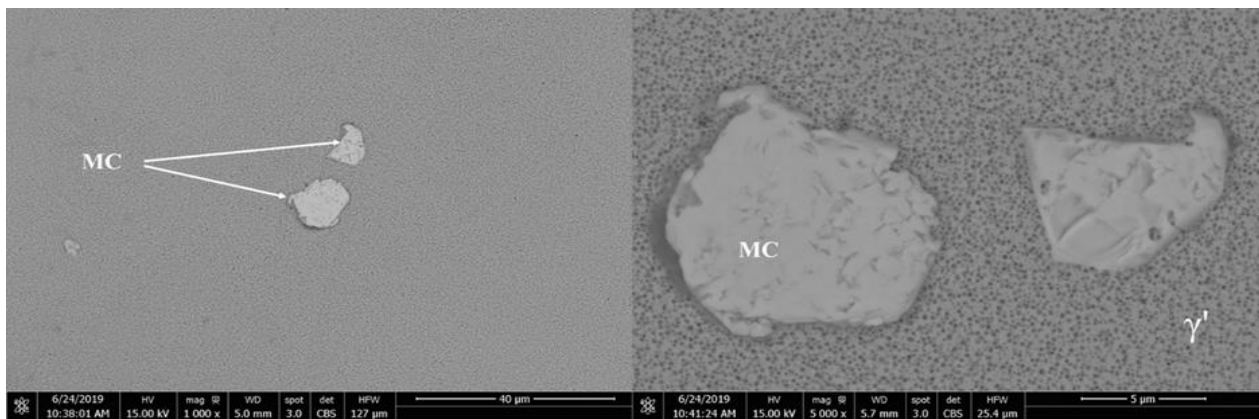


Figure 7. SEM image—the microstructure of GTD111 after the aging heat treatment process

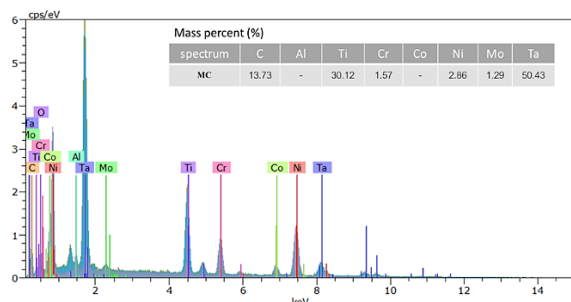
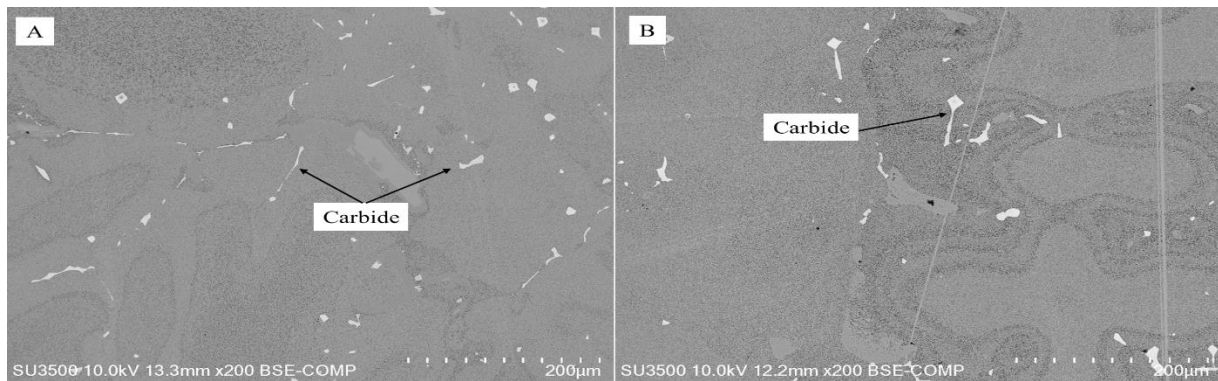


Figure 8. Quantitative analysis of particle composition by EDS

which is scattered along the line, continues to have a carbide structure on the  $\gamma'$  and  $\gamma$  phases. The chemical composition of the primary MC carbides in the heat-treated alloy measured is illustrated in Figure 8. The main elements forming the primary MC carbides are Ti and Ta; the MC carbides show little morphological change after reheat treatment. Figure 9B shows the primary aging temperature of 1120 °C for 3 h and secondary aging temperature at 890 °C for 24 h. The SEM scattered image of the carbide structure with  $\gamma'$  precipitate with a different size. The dispersion of these constituents formed from non-equilibrium solidification can degrade the tensile



**Figure 9.** SEM of GTD111 grade after the heat treatment process. A. primary aging temperature of 1,120 °C for 3 h., secondary aging temperature of 845 °C for 24 h. B. Primary aging temperature of 1,120 °C for 3 h., secondary aging temperature of 890 °C for 24 h

properties at high temperatures. The reheat-treated alloy was dangerous as it risked causing intergranular fracture along the grain boundaries, where the  $\gamma'$  precipitates are rafted and in the interdendritic region where MC carbides are located. However, cracking can form at the interdendritic region; some cracks also grew in the  $\gamma'$  phase, which indicated bigger grain boundary strengths than reported in the corresponding results of Long [23] and Berahmand [24]. The different parameters after the heat treatment process of Ni-base superalloy grade GTD 111 can influence variations in the microstructure and mechanical properties.

The aim of the experiment was to improve the hardness and microstructure with the heat treatment process according to the 27 samples of the Taguchi experiment design, then test the microstructure with SEM and EDS. Low heat input in primary heat treatment with a primary aging temperature of 1050 °C for 1 h. and secondary aging temperature of 800 °C for 22 h. found that the small spherical and square shapes of the  $\gamma'$  particle were small, with a size of 0.086  $\mu\text{m}$ , and the  $\gamma'$  particle precipitate was evenly distributed on the  $\gamma$  phase, as shown in Figure 10A. The samples tested with a primary aging temperature of 1087 °C for 2 h. and secondary aging temperature of 845 °C for 26 h. found that for the  $\gamma'$  size of 0.270  $\mu\text{m}$ , the particle characteristics were a coarse square shape of  $\gamma'$  and an evenly distributed precipitate, as shown in Figure 10B. In the SEM microstructure in Figure 10C, with a primary aging temperature of 1120 °C for 3 h. and secondary aging temperature of 845 °C for 24 h. A coarse square shape, spherical shape of  $\gamma'$  and fine  $\gamma'$  precipitate distributed on the parent phase was found, in agreement with previous studies of Zhang [25]. At a secondary aging increase of 890 °C, where the coarse  $\gamma'$  of square shape increased in size, there was a fine distribution of  $\gamma'$  in the less dense parent phase, as shown in Figure 10D. The result of over-aging temperature causing the lowest hardness of all of the GTD111 is in

accordance with the research of Wang [25] and Zhanga [26], who reported that the increase in the secondary aging temperature results in an increase on the coarse  $\gamma'$  size, which affects the mechanical properties of the material.

**3. 4. Hot Tensile Analysis** The material GTD111 was used at temperatures between 750 and 900 °C in the combustion chamber of the jet engine [27]. According to the research, once the mechanical properties and microstructural refurbishment of the GTD111 material were modified with rejuvenation heat treatment, it was necessary to conduct tests to confirm the feasibility of using heat-treated materials with hot tensile strength tests. The hot tensile strength test was selected for the optimum conditions from the Taguchi experiment at a primary aging temperature of 1120 °C for 3 h. and secondary aging temperature of 845 °C for 24 h. The specimen with the lowest hardness at a primary aging temperature of 1050 °C for 1 h. and secondary aging temperature of 800 °C for 22 h. was tested at 871 °C, in accordance with ASTM E8.

The hot tensile test showed that for the GTD111 grade, in an optimization condition of primary aging temperature of 1120 °C for 3 h. and secondary aging temperature of 845 °C for 24 h. The specimen had a higher strength at 402 MPa. A comparison was run with a GTD111 heat treatment with a primary aging temperature of 1050 °C for 1 h and secondary aging temperature of 800 °C for 22 h, and the tensile strength was found to be 316 MPa. Figure 11A shows the fracture mechanism, which shows rather brittle characteristics, and GTD111 also has a continued cleavage fracture behavior in the microcrack area. This fracture mode was associated mainly with the secondary phase. Dadkhah and Kermanpur [28] also reported corresponding results, such as that the primary aging temperature changed the fracture mode from ductile to rather brittle and also

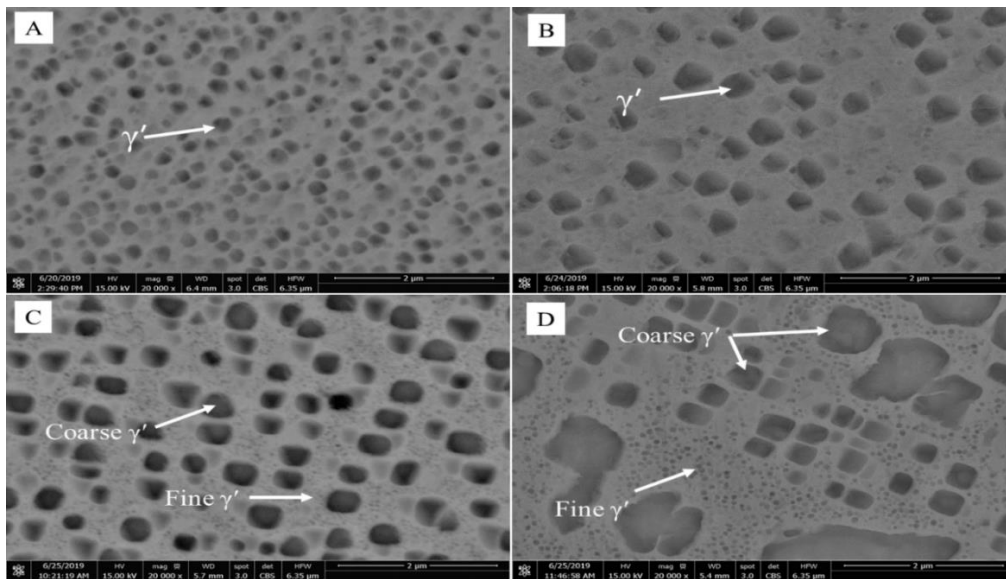


**Figure 10.** SEM image—the microstructure of GTD111 after heat treatment process. A. Primary aging temperature of 1,050 °C for 1 hr, secondary aging temperature of 800 °C for 22 h. B. Primary aging temperature 1,087 °C for 2 h., secondary aging temperature of 845 °C for 26 h. C. Primary aging temperature of 1,120 °C for 3 h., secondary aging temperature of 845 °C for 24 h. D. Primary aging temperature of 1,120 °C for 3 h., secondary aging of 890 °C for 24 h

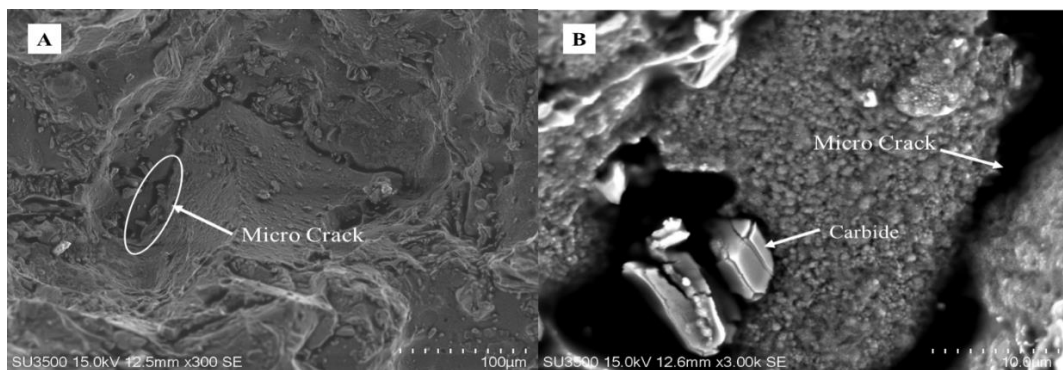


**Figure 11.** Fracture surface of GTD111 after a hot tensile test of 871 °C

consistent with the higher hardness in the specimen. This is also consistent with the findings of Sajjadi et al. [29], who studied tensile deformation mechanisms at different temperatures in the Ni-base superalloy GTD-111, which resulted in hot tensile deformation and led to growth of  $\gamma'$  particles normal and carbide in the load direction. Figure 11 (B) shows a zoomed image of the fracture area, where it was found that the MC carbides are near the micro crack. The negative lattice misfit of  $\gamma/\gamma'$  and the position of the carbide had an effect on the loading direction in the hot tensile test [30]. The MC carbide in the thermally exposed alloy resulted in cracks being formed along the grain boundaries, which is similar to the corresponding results of Choi et al. [31]. The behavior in carbide phases resulted in fractures after the hot tensile test because primary MC carbides were scattered within the grain interiors as well as along the grain boundaries.

#### 4. CONCLUSION

This research work examines the effects of heat treatment on grade GTD111 after long-term service using optimization with Taguchi method. Primary aging temperature, primary aging time, secondary aging temperature, and secondary aging time were taken as input heat treatment variables and appraised in terms of mechanical property and microstructure. The research study highlights the following outcomes based on the experiments:

1. Taguchi design method is suitable to analyze and optimize the heat treatment parameters as described in the best parameters of hardness and hot tensile test for optimization, with a primary aging temperature of 1120 °C, primary aging time of 3 h, secondary aging temperature of 845 °C, and secondary aging



time of 24 h. The regression model for the hardness of the collected data was approximately 83.72% ( $R^2_{adj}$ ), which shows that the response can be described by the experimental factors;

- The predicted hardness values that were obtained using a regression model were consistent with the experimental values as follows:  $Y_{HV} = 220 + 0.279(X_1) + 3.880(X_2) - 0.0362(X_3) + 0.414(X_4)$ ;
- In the Ni-based superalloys grade GTD111, after rejuvenation heat treatment, the gamma prime particle ( $\gamma'$  or Ni<sub>3</sub>(Al,Ti)) precipitate was found to be evenly distributed on the gamma ( $\gamma$ ). The EDS test showed additional related elements of discontinuous MC carbides (Ta,Ti,W), and the carbide layer was scattered throughout the matrix;
- The size and shape of precipitates of  $\gamma'$  and carbide phase was controlled through the heat treatment process. In the optimization condition with the  $\gamma'$  particle, the characteristics were a coarse square shape and spherical shape of  $\gamma'$  and fine  $\gamma'$  precipitate distributed on the parent phase, which affects the mechanical properties of the material.
- Rejuvenation of GTD111 by heat treatment can restore the mechanical properties and microstructure to their status before their long-term service began when the hot tensile test has a tensile stress of 402 MPa. It was found that high-temperature rupture of the material with suitable conditions caused a micro crack at the position of the carbide, which resulted in the material being brittle.

## 5. ACKNOWLEDGEMENT

This research supported by the Petch Pra Jom Klaw Master's Degree Research Scholarship from King Mongkut's University of Technology Thonburi.

## 6. REFERENCES

- A.B. Esanab, V. Ehiaguinab, C. Awosopeb, L. Olatomiwac and D. Egbunea, "Data-based investigation on the performance of an independent gas turbine for electricity generation using real power measurements and other closely related parameters", *Data in Brief*, Vol. 26, (2019), 1-16, <https://doi.org/10.1016/j.dib.2019.104444>.
- Matthew J. et al. 2002, *Superalloy A Technical Guide*, ASM International Publications, Ohio, 2000.
- J.R. Davis, *ASM specialty Handbook Nickel Cobalt and Their Alloy*, ASM International Publications, Ohio, 2000.
- M. Perrut, P. Caron, M. Thomas and A. Couret., "High temperature materials for aerospace applications: Ni-based superalloys and  $\gamma$ -TiAl alloys", *Comptes Rendus Physique*, Vol. 19, (2018), 657-671, <https://doi.org/10.1016/j.crhy.2018.10.002>.
- B. Salehnasab, E. Poursaeidi, S.A. Mortazavi and G.H. Farokhian, "Hot corrosion failure in the first stage nozzle of a gas turbine engine", *Engineering Failure Analysis*, Vol. 60, (2016), 316-325, <https://doi.org/10.1016/j.engfailanal.2015.11.057>.
- P. Zhangab, J. Lic, X. F. Gongd, Y. Yuana, Y.F. Gua, J.C. Wangb, J.B. Yana and H.F. Yina, "Creep behavior and deformation mechanisms of a novel directionally solidified Ni-base superalloy at 900°C", *Materials Characterization*, Vol. 148, (2019), 201-207, <https://doi.org/10.1016/j.matchar.2018.12.023>.
- J.K. Kim, H.J. Park, D.N. Shim and D.J. Kim, "Transient liquid phase bonding of  $\gamma'$ - precipitation strengthened Ni based superalloys for repairing gas turbine components", *Journal of Manufacturing Processes*, Vol. 25, (2017), 60-69, <https://doi.org/10.1016/j.jmappro.2016.10.002>.
- A. Rezaie and S.E. Vahdat, "Study of effects of temperature and pressure in HIP process on mechanical properties of nickel-based superalloys", *Materials Today Proceeding*, Vol. 4, (2017), 152-156, <https://doi.org/10.1016/j.matpr.2017.01.008>.
- X.W. Jiang, D.Wang, Di.Wang, H.Li and L.H.Lou, "The effect of reheat treatment on microstructure and stress rupture property of a directionally solidified nickel-based superalloy after long-term thermal exposure", *Materials Science and Engineering: A*, Vol. 694, (2017), 48-56, <https://doi.org/10.1016/j.msea.2017.03.116>.
- Y.Y. Kaplanskii, E.A. Levashov, A.V. Korotitskiy, P.A. Loginov, Zh. A. Sentyurina and A.B. Mazalov, "Influence of aging and HIP treatment on the structure and properties of NiAl-based turbine blades manufactured by laser powder bed fusion", *Additive Manufacturing*, Vol. 31, (2020), 1-12, <https://doi.org/10.1016/j.addma.2019.100999>.
- J. Xua, H. Gruberb, D. Denga, R. Lin, P. Johan and J. Moverarea, "Short-term creep behavior of an additive manufactured non-weldable Nickel-base superalloy evaluated by slow strain rate testing", *Acta Materialia*, Vol. 179, (2019), 142-157, <https://doi.org/10.1016/j.actamat.2019.08.034>.
- C.D. Pimenta, M.B. Silva, R.L. de Moraes Campos, and W.R. de Campos Junior, "Application of the Taguchi method in the investigation of influential heat treatment factors in steel wires", *International Journal of Innovative Research and Development*, Vol. 8, (2019), 111-114, <https://doi.org/10.24940/ijird/2019/v8/i3/MAR19029>
- H. Terzioglu, "Analysis of effect factors on thermoelectric generator using Taguchi method", *Measurement*, Vol. 149, (2019), 1-10, <https://doi.org/10.1016/j.measurement.2019.106992>.
- G. kartheek, K. Srinivas and Ch. Devaraj, "Optimization of residual stresses in hard turning of super alloy inconel 718, Materials today: Proceedings", *Materials today: Proceedings*, Vol. 15, (2018), 4592-4600, <https://doi.org/10.1016/j.matpr.2017.12.029>.
- A. Kumar, A.R. Ansari, B. N. Roy, and S. Kumar, "Heat treatment parameter optimization using Taguchi technique", *International Journal of Scientific Research and Education*, Vol. 4, (2016), 5965-5974, <https://doi.org/10.18535/ij sre/v4i10.07>.
- R.M. Dodo, T. Ause, E.T. Dauda, U. Shehu and A.P.I. Popoola, "Multi-response optimization of transesterification parameters of mahogany seed oil using grey relational analysis in Taguchi method for quenching application", *Helicon*, Vol. 5, (2019), 1-7, <https://doi.org/10.1016/j.heliyon.2019.e02167>.
- M. Sobhani, H. Ahmadi, T. Javad and A. Esfahani, "Taguchi optimization of combined radiation/natural convection of participating medium in a cavity with a horizontal fin using LBM", *Physica A: Statistical Mechanics and its Applications*, Vol. 509, (2018), 1062-1079, <https://doi.org/10.1016/j.physa.2018.06.056>.
- A.S. Canbolata, A.H. Bademlioglu, N. Arslanoglu and O. Kaynaklia, "Performance optimization of absorption refrigeration systems using Taguchi, ANOVA and grey relational analysis

- methods”, *Journal of Cleaner Production*, Vol. 229, (2019), 874-885, <https://doi.org/10.1016/j.jclepro.2019.05.020>.
19. J.A. Daleo and J.R. Wilson, “GTD111 alloy material study”, *Journal of Engineering Gas Turbines Power*, Vol. 120, (2013), 375-382, <http://doi:10.1.1.875.4753&rep=rep1&type=pdf>.
  20. A. Rezaie and S. E. Vahdata, “Study of effects of temperature and pressure in HIP process on mechanical properties of nickel-based superalloys”, *Materials Today: Proceedings*, Vol. 4, (2017), 152-156, <https://doi.org/10.1016/j.matpr.2017.01.008>.
  21. Kathleen Mills, *ASM Handbook Volume 9 Metallography and Microstructures*, ASM International Publications, Ohio, (1985)
  22. John N. Dupont, *Welding Metallurgy and weldability of nickel base alloy*, A John Wiley and Son Publishing, New Jersey, (2009)
  23. F. Long, Y.S. Yoo, C.Y. Jo, S.M. Seo, Y.S. Song, T. Jin and Z.Q. Hu, “Formation of  $\eta$  and  $\sigma$  phase in three polycrystalline superalloys and their impact on tensile properties”, *Materials Science and Engineering A*, Vol. 527, (2009), 316-369, <https://doi.org/10.1016/j.msea.2009.09.016>.
  24. M. Berahmand and S. A. Sajjadi, “Morphology evolution of  $\gamma'$  precipitates in GTD-111 Ni-based superalloy with heat treatment parameters”, *International Journal of Materials Research*, *International Journal of Materials Research*, Vol. 104, (2013), 275-280, <https://doi.org/10.3139/146.110856>.
  25. Q. Wang, Z. Li, S. Pang, X Li, C Dong and P. K. Liaw, “Coherent precipitation and strengthening in compositionally complex alloys: A Review”, *Entropy*, Vol. 20, (2018), 1-23, <https://doi.org/10.3390/e20110878>.
  26. P. Zhanga, Y. Yuan, J. Li, Y.F. Xu, X.L. Song and G.X. Yang, “Tensile deformation mechanisms in a new directionally solidified Ni-base superalloy containing coarse  $\gamma'$  precipitates at 650 °C”, *Materials Science and Engineering A*, Vol. 702, (2017), 343-349, <https://doi.org/10.1016/j.msea.2017.07.025>.
  27. M. Vinoth Kumar, V. Balasubramanian and A. Gourav Rao, “Hot tensile properties and strain hardening behavior of super 304HCu stainless steel”, *Journal of Materials Research and Technology*, Vol. 6, (2016), 116-122, <https://doi.org/10.1016/j.jmrt.2016.05.004>.
  28. A. Dadkhah and A. Kermanpur, 2017, “On the precipitation hardening of the directionally solidified GTD-111 Ni-base superalloy: Microstructures and mechanical properties”, *Materials Science and Engineering A*, Vol. 685, (2017), 79-86, <https://doi.org/10.1016/j.msea.2017.01.005>.
  29. S. A. Sajjadi, S. Nategh, M. Seyed, and M. Zebarjad, “Tensile deformation mechanisms at different temperatures in the Ni-base superalloy GTD-111”, *Journal of Materials Processing Technology*, Vol. 155-156, (2004), 1900-1904, <https://doi.org/10.1016/j.jmatprotec.2004.04.273>.
  30. L. Zhang, Y. Zhou, X. Jin, X. Du and B. Li, “The microstructure and high-temperature properties of novel nano precipitation-hardened face centered cubic high-entropy superalloys”, *Scripta Materialia*, Vol. 146, (2018), 226-230, <https://doi.org/10.1016/j.scriptamat.2017.12.001>.
  31. B. G. Choi, I. S. Kim, D. H. Kim and C. Y. Jo, “Temperature dependence of MC decomposition behavior in Ni-base superalloy GTD 111”, *Materials Science and Engineering A*, Vol. 478, (2008), 343-349, <https://doi.org/10.1016/j.msea.2007.06.010>.

---

### Persian Abstract

#### چکیده

این تحقیق یک بهینه سازی و جوان سازی فرآیند عملیات حرارتی برای درجه فوق العاده آلیاژ پایه نیکل GTD111 را پس از خدمات طولانی مدت توصیف می کند. متغیرهای عملیات حرارتی پیری بررسی شده در این مطالعه شامل دمای پیری اولیه، زمان پیری اولیه، دمای پیری ثانویه و زمان پیری ثانویه است. مواد بدست آمده با استفاده از روش آزمایش تاگوچی آزمایشات تعیین شد تا آزمایش سختی ماده حاصل شود و با آزمایش کشش گرم، میکروسکوپ الکترونی روبشی و طیفسنجی اشعه X پراکندگی انرژی مشاهده شد. نتایج تجربی نشان داد که در پی بهینه سازی با پارامترهای عملیات حرارتی دمای پیری اولیه ۱۱۲۰ درجه سانتیگراد، زمان پیری اولیه ۳ ساعت، دمای پیری ثانویه ۸۴۵ درجه سانتیگراد و زمان پیری ثانویه ۲۴ ساعت چه اتفاقی می افتد. این ماده، پس از عملیات حرارتی جوان سازی از طریق بهینه سازی با ویژگی های ذرات  $\gamma'$ ، دارای یک شکل مربع درشت، شکل کروی  $\gamma'$ ، و رسوب  $\gamma$  fine خوب توزیع شده بر روی فاز اصلی است، که بر خصوصیات مکانیکی مواد تأثیر می گذارد. رسوب خوب  $\gamma$  distributed توزیع شده بر روی فاز اصلی، که بر خصوصیات مکانیکی مواد تأثیر می گذارد.

---